Effects of Nanoparticles on the Density Reduction and Cell Morphology of Extruded Metallocene Polyethylene/ Wood Fiber Nanocomposites

G. Guo, K. H. Wang, C. B. Park, Y. S. Kim, G. Li

Microcellular Plastics Manufacturing Laboratory, Department of Mechanical and Industrial Engineering, University of Toronto, Toronto, Ontario, Canada M5S 3G8

Received 27 October 2006; accepted 6 June 2006
DOI 10.1002/app.25778
Published online in Wiley InterScience (www.interscience.wiley.com).

ABSTRACT: This article investigates the effects of nanoparticles on cell morphology and foam expansion in the extrusion foaming of metallocene polyethylene/wood fiber nanocomposites with a chemical blowing agent. The results indicate that the addition of clay generally reduces the cell size, increases the cell density, and facilitates foam expansion. Furthermore, the foam material with added clay shows good char formation when it is burned. © 2007 Wiley Periodicals, Inc. J Appl Polym Sci 104: 1058–1063, 2007

Key words: blowing agents; extrusion; flame retardance; morphology; nanocomposites

INTRODUCTION

The fine-celled foaming of plastic/wood fiber composites (PWCs) has increased the applications of PWCs[1–4] by producing a number of benefits, such as reduced weight, lowered cost, and improved impact strength. The expanding markets, however, call for high-performance PWCs with superior and unique properties (e.g., flame retardance) to meet individual application requirements. Compared with conventional polyethylene, metallocene polyethylene (mPE) offers better mechanical properties, including toughness, puncture resistance, and impact strength. Therefore, mPE could be a good base material for improving the mechanical properties of PWCs.

The use of layered silicate nanoparticles (i.e., clays) to reinforce polymers has drawn a great deal of attention in recent years.[5–10] Adding a small amount of clay can dramatically improve a number of properties, such as the tensile modulus and strength, flexural modulus and strength, impact strength, thermal stability, flame retardance, and barrier properties.[8–10] Thus, the introduction of clay into PWC could prove interesting from the perspective of improving the mechanical properties and flame retardance, which is desirable, particularly with respect to construction applications.

This research explores the effects of nanoparticles on cell morphology and foam expansion in the foaming of mPE/wood fiber (WF) nanocomposites with a single-screw extrusion system. The crystallinity, solubility, and diffusivity of mPE, mPE nanocomposites, and their PWCs were measured to elucidate further the foam-expansion mechanism. The overall effects of the nanoparticles on the crystallinity, solubility, and diffusivity of the composites were also studied more generally.

EXPERIMENTAL

Materials

The plastic material used in this study was mPE (8490, Dupont Dow Elastomers L. L. C. (Wilmington, DE); melt flow index = 7.5), which was filled with 5 wt % nanoclay (Cloisite 20A, Southern Clay Products, Inc., Austin, TX) by the melt-blending method.[8,9] The WF used was standard softwood (pine), grade 12020, and was supplied by American Wood Fibers (Columbia, MD). A coupling agent (CA), Fusabond adhesive resin E-MB226D from Dupont Canada (Mississauga, Canada), was used for improving the adhesion between the hydrophobic mPE and the hydrophilic WF. The chemical blowing agent (CBA), ABC 2750 from Endex, Inc. (Ajax, Canada), that was used in this study had an onset decomposition temperature of 133°C. All the materials were used as received.

Table I shows the formulations of the materials for this study. The WF content had two levels: 30 and 50%.

Correspondence to: C. B. Park (park@mie.utoronto.ca).
Contract grant sponsor: Materials and Manufacturing Ontario.
Contract grant sponsor: Andersen Corp.
Contract grant sponsor: Brite Manufacturing, Inc.
Contract grant sponsor: CertainTeed Corp.
Contract grant sponsor: Dupont Canada, Inc.
Contract grant sponsor: Imperial Building Products, Inc.
Contract grant sponsor: Plastic Lumber Co., Inc.

Journal of Applied Polymer Science, Vol. 104, 1058–1063 (2007)

TABLE I
Formulations of the Materials

	Formulation	WF (wt %)	Base plastic (wt %)	CBA (% of total weight)
mPE	1	30	70	0
	2	30	70	1
	3	50	50	0
	4	50	50	1
mPE nanocomposites (5% clay filled)	5	30	70	0
	6	30	70	1
	7	50	50	0
	8	50	50	1

Preparation of the mPE/clay nanocomposites

First, the mPE/clay nanocomposites were prepared with a W&P ZSK30 corotating (Stuttgart, Germany), intermeshing twin-screw extruder (length/diameter = 38 : 1, diameter = 30 mm). The screw rotating speed was 250 rpm, and the extrusion temperature was 150°C. The clay content was fixed at 5 wt %, and the CA content was fixed at 10 wt %, which is the amount of CA typically used to improve the dispersion of clay in an mPE matrix.

Second, the nanocomposite structure was characterized by wide-angle X-ray diffraction (WAXD). WAXD was conducted with a Siemens D5000 diffractometer (Karlsruhe, Germany) with Cu Kα radiation (1.5478 Å) with a Kevex solid-state detector. Measurements were performed at 50 kV and 35 mA. The data were recorded in the reflection mode in the range of $2\theta = 1.5–10^\circ$ with the step-scan mode. The step size was 0.02°, and the counting time was 2.0 s per step.

Studies on the crystallization behavior of the nanocomposites

The crystallization temperature and crystallinity of the specimens were investigated with a TA Instruments 2910 differential scanning calorimeter (New Castle, DE) at a scanning rate of 10°C/min under a nitrogen environment. Sample weights of 4–6 mg were used in all the tests. The crystallinity was calculated from the specific heat required for melting by the integration of the corresponding peak and the division of this value by the heat of fusion for the pure crystalline phase of polyethylene (293 J/g).[11]

Solubility and diffusivity studies

The solubility and diffusivity of the composites were measured with a magnetic suspension balance. Because the WF would release gaseous volatiles at the processing temperature (i.e., typically 150°C[12,13]), it was difficult to measure the solubility under the processing conditions. Therefore, a temperature of 30°C and a pressure of 650 psi were chosen as the measuring conditions.

Foaming setup and procedure

The WF was dried at 105°C for 6 h in a vacuum oven to remove any inherent moisture and thereby prevent the deteriorating effects of moisture on the cell structure.[12,13] The dried WF, the base resin (mPE or mPE nanocomposite), and the CA were blended with a K-mixer[14] and then granulated. The PWC granules were then processed in a counter-rotating twin-screw compounder [Fig. 1(a)]. The temperature throughout the extruder was maintained at 175°C to thoroughly devolatilize the extrudate. The extrudate was cooled by air blowing over it, and it was fed into a pelletizer to obtain PWC pellets. Moreover, all the vaporized water and other volatiles released into the barrel of the twin-screw extruder were purged out to the atmosphere so that only moisture-free extrudates would be pelletized.

The PWC pellets were dry-blended with a CBA and processed in a single-screw, three-zone extruder [Fig. 1(b)]. For the case processed without a CBA, the temperature in this extruder was maintained at 105, 115, and 140°C in zones 1, 2, and 3, respectively. For the CBA-based process, the extruder temperatures were 105, 115, and 155°C in zones 1, 2, and 3, respectively. The CBA decomposed mostly in zone 3, and the released gases were trapped and dispersed in the extrudate. A static mixer, a heat exchanger, and a filament die (length/diameter = 0.22 : 0.0635) were attached to the barrel in the downstream. Their temperatures were set at 155, 145, and 140°C, respectively. The die temperature was reduced at intervals of 5°C, from 140°C to a lower temperature, to prevent gas loss. Starting at 140°C, samples

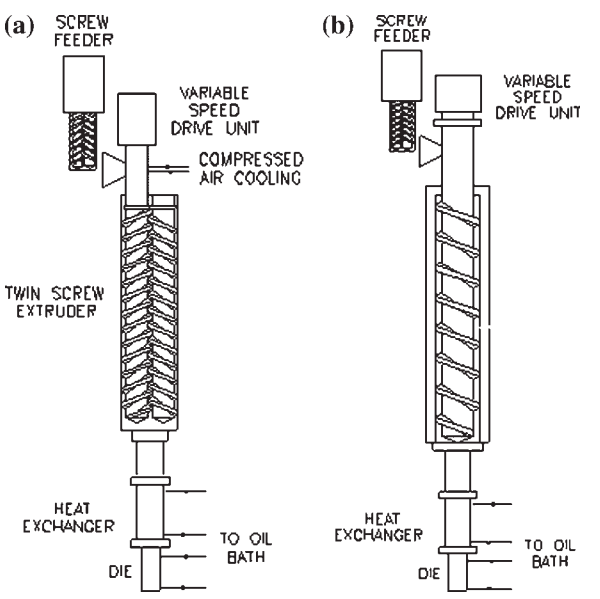

Figure 1 Experimental setup: (a) with a twin-screw extruder and (b) with a single-screw extruder.

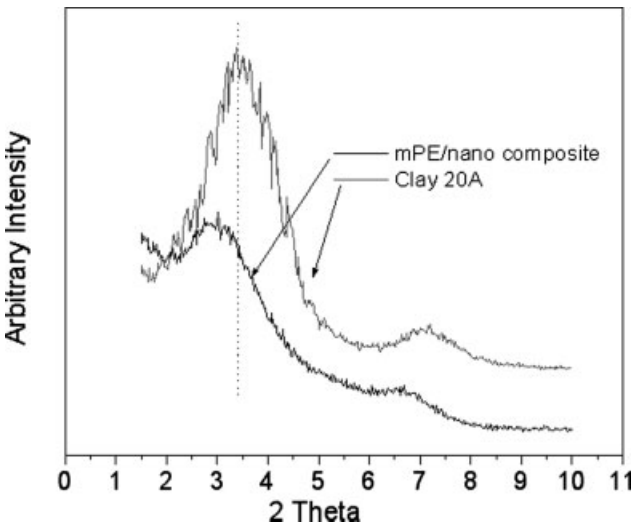

Figure 2 XRD patterns for the mPE/clay nanocomposite and clay.

were collected at each 5°C interval when the stable processing conditions were attained.

This two-stage processing method was adopted to avoid CBA decomposition during the high-temperature devolatilizing procedure in the first extruder. The intent was to maintain the highest processing temperature below 160°C so as to maximize the effects of the CBA on density reduction while minimizing the contribution of the volatile emissions from the WF.

The foam samples were randomly collected under each stabilized processing condition and characterized for the foam density and cell morphology. To determine the cellular morphology, each sample was first dipped in liquid nitrogen and subsequently fractured. The fractured surface was then gold-coated, and the microstructure was examined with a Hitachi 510 scanning electron microscope (Schaumburg, IL).

RESULTS AND DISCUSSION

Structure of the mPE/clay nanocomposites

The structure of the mPE nanocomposites was examined with X-ray diffraction (XRD). Figure 2 shows the XRD patterns of the mPE/clay nanocomposites used in this study. There was a weak peak at the lower angle of the nanocomposites in comparison with the pure clay. The pattern indicated that the nanocomposites had an intercalation morphology in the mPE matrix.

Effects of the nanoparticles on foam expansion

Figure 3 shows that when the nanoparticles were introduced into PWC for both the 30 and 50% WF cases, the density of the composites decreased, regardless of the CBA effects. One contributing factor could have been that the nanoparticles were well dispersed in the plastic matrix and thus increased the melt stiffness, thereby reducing the gas diffusivity. Because the gas diffusivity was reduced, the possibility of gas escape from the extrudate skin was also reduced.

Without the addition of CBA, the density was reduced when nanoparticles were added. This indicated that drying WF at 105°C for 6 h could not completely remove the volatiles. When the processing temperature (145°C) was higher than the drying temperature, the WF still released the gaseous volatiles, which contributed to the density reduction.

When 1% CBA was added in each case, the foam density was reduced. The mPE nanocomposites, however, underwent a much larger density reduction than the mPE composites. This was indicated by the bigger gap between the curve without CBA and the curve with CBA for the mPE/WF nanocomposite case.

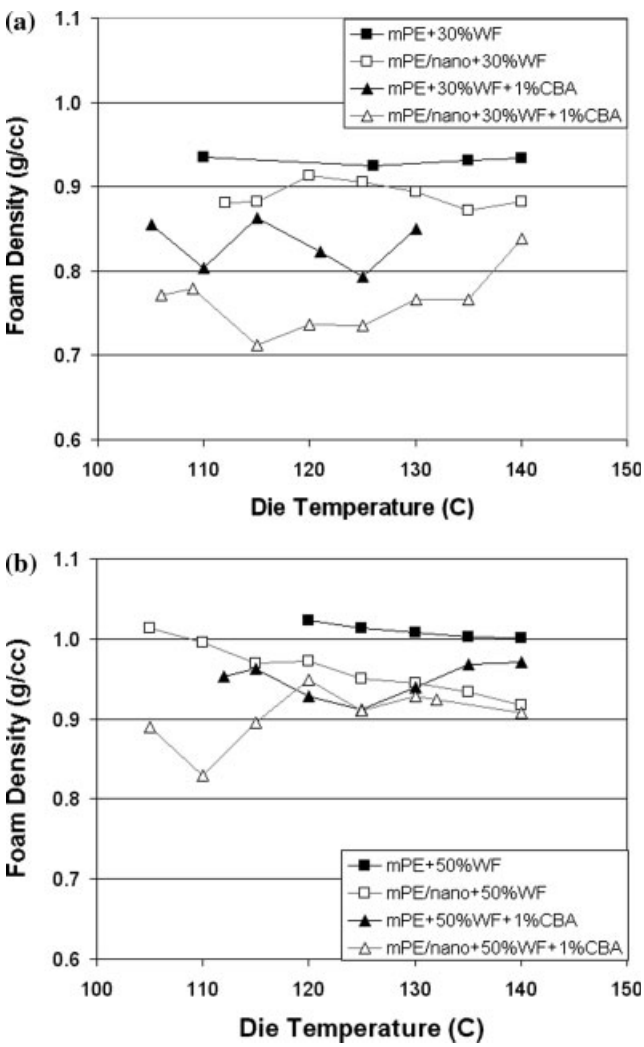

Figure 3 Foam density versus the die temperature: (a) 30 and (b) 50% WF.

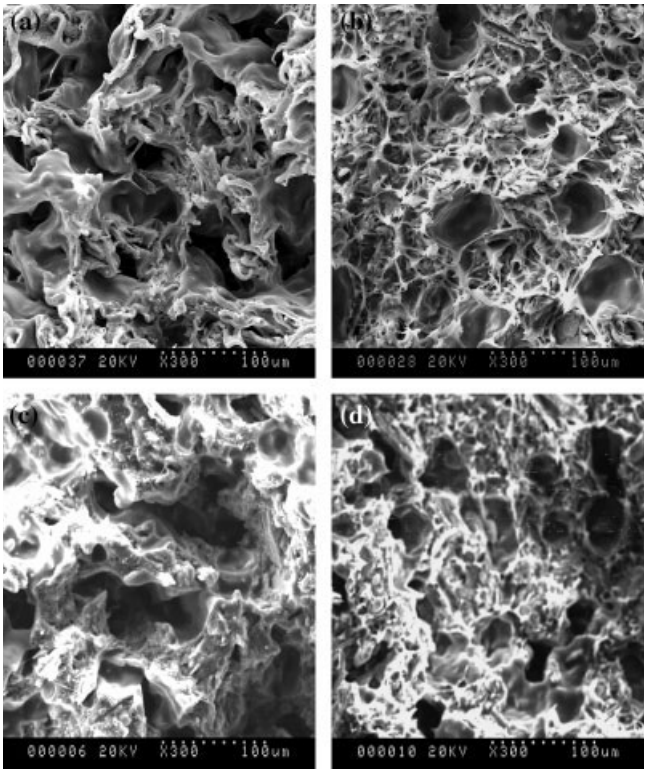

Figure 4 Scanning electron microscopy pictures of mPE/WF composite foams with 1% CBA at the die temperature of 125°C: (a) mPE/30% WF composite, (b) mPE/30% WF nanocomposite, (c) mPE/50% WF composite, and (d) mPE/50% WF nanocomposite.

Effects of the nanoparticles on the cell morphology

The effects of the nanoparticles on the cell morphology were investigated (Fig. 4). With the addition of 5 wt % nanoparticles, the PWC generally had a smaller cell size and more cells per unit of volume. Although the cell nucleation and deterioration mechanisms for PWCs with nanoparticles have not been clarified yet, it is clear that the addition of nanoparticles increases the nucleation rate on the basis of heterogeneous nucleation.[7,15] In the heterogeneous nucleation scheme, the activation energy barrier to nucleation is sharply reduced in the presence of filler particles. This increases the nucleation rate and hence the number of bubbles produced. However, further study is required to identify the exact mechanisms of cell nucleation (and cell deterioration if any) for PWCs. The role of nanoclay in enhancing the cell nucleation and/or suppressing cell deterioration will also need to be identified.

Crystallization temperature, crystallinity, solubility, and diffusivity for the mPE, mPE nanocomposites, and their PWCs

Table II shows the crystallization temperature, crystallinity, solubility, and diffusivity for mPE, mPE

TABLE II
Crystallization Temperature, Crystallinity, Solubility, and Diffusivity Values of the mPE/WF Composites, mPE Nanocomposites, and mPE/WF Nanocomposites

Sample	Crystallization temperature (°C)	Crystallinity of the composite (%)	Crystallinity of the polymer (%)[a]	Solubility (g of gas/g of composite)	Solubility (g of gas/g of polymer)[a]	Diffusivity (cm^2/s)
mPE	86.65	34.56	34.56	0.03092	0.03092	11.7×10^{-7}
mPE nanocomposite (5% Clay)	91.33	32.18	33.87	0.03063	0.03222	8.0×10^{-7}
mPE/30% WF composite	87.98	28.47	40.67	0.02891	0.04130	6.3×10^{-7}
mPE/30% WF nanocomposite (3.5% Clay)	91.76	20.43	30.72	0.02847	0.04217	4.8×10^{-7}
mPE/50% WF composite	88.58	15.12	30.24	0.02756	0.05512	2.6×10^{-7}
mPE/50% WF nanocomposite (2.5% Clay)	89.27	10.95	23.05	0.02626	0.05528	2.8×10^{-7}

[a] These data were calculated with the measured data.

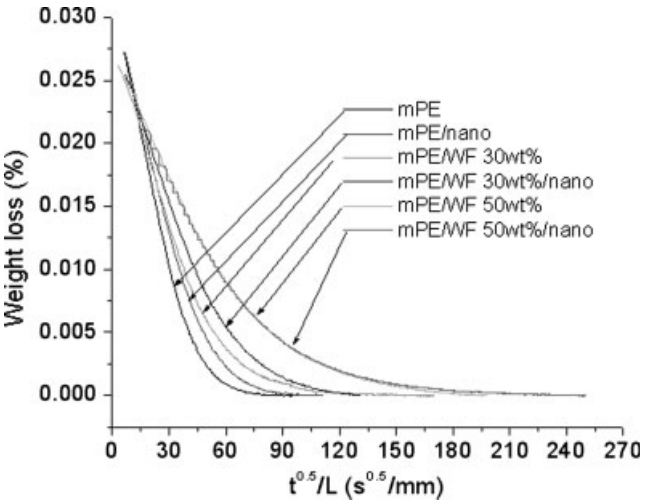

Figure 5 Diffusivity of mPE composites, mPE nanocomposites, and mPE/WF nanocomposites.

nanocomposites, mPE/WF composites, and mPE/WF nanocomposites.

Crystallization temperature and crystallinity

Metallocene PE is a semicrystalline polymer, and its mechanical properties are greatly affected by its overall crystallinity. The foaming behavior of a semicrystalline polymer largely depends on the crystallization temperature.[16] Therefore, it is important to investigate the effects of clay on the crystallization behavior of mPE. The measured crystallization temperature and crystallinity of the different mPE/WF nanocomposites are shown in Table II. The crystallization temperatures of all PWCs increased when the clay was added, and this indicated that the crystal nucleation occurred faster because of the nucleating role of clay and WF for the crystallites. The crystallinity decreased as the WF content increased, except for mPE/WF with 30 wt % WF. This could be because of the lowered mobility of polymer chains in the PWC matrix, which resulted from the presence of dispersed WF and clay particles. The presence of these dispersed particles prevented large crystalline domains from forming in the restricted space. For pure mPE, the addition of clay had a small effect on the crystallinity of mPE. However, for the mPE/WF composites, the addition of clay significantly reduced the crystallinity of mPE.

Solubility and diffusivity

Figure 5 shows the CO_2 desorption curves for the samples. The initial stage of the desorption curve of CO_2 from the polymer is linear with respect to time,[17] and the y intercept back to time zero yields the solubility of the samples of the experiment. By extrapolation from the desorption curve, the solubility of CO_2 of all PWCs was calculated and is shown in Table II.

The solubility of CO_2 in a semicrystalline polymer depends strongly on the crystallinity of that polymer.[18,19] It seems that the higher solubility in the mPE nanocomposites was due to the lower crystallinity compared with that of the mPE composites. However, for all PWCs, the addition of WF seems to have played a more significant role in increasing the solubility. It is hypothesized that the addition of WF to the polymer matrix introduced some void either from the interfacial area between the WF and polymer matrix or from the WF itself (i.e., hollow voids in the cellular wood structure, which had not completely collapsed during processing). The void volume could have increased the capacity for accommodating more gas molecules and thereby increased the solubility. Further studies on the effect of WF on the solubility and diffusivity will be conducted in the future to clarify this hypothesis.

The diffusivities of CO_2 in the samples were determined with the following equation for Fickian diffusion[20] through a flat plate:

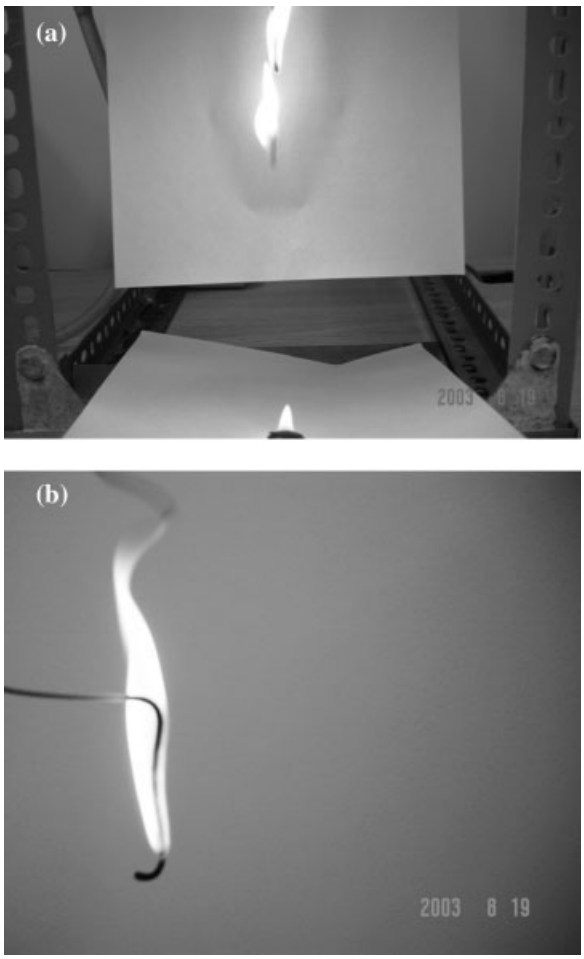

Figure 6 Burning test of mPE/WF composite foams (a) without clay and (b) with 5 wt % clay.

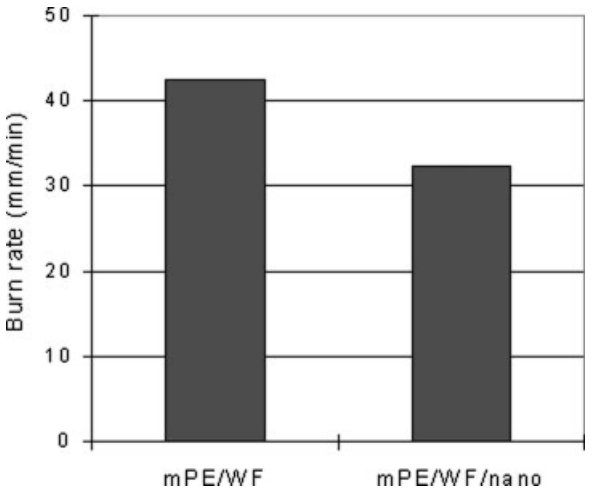

Figure 7 Burning rates of the mPE/WF composites and mPE/WF nanocomposites.

$$M_t/M_\infty = 4(D/\pi)^{0.5}(t^{0.5}/L) \quad (1)$$

where M_t is the mass gain by the sample at time t, M_∞ is the maximum mass gain, D is the diffusivity of CO_2 in the polymer, and L is the thickness of the sample. M_∞ is the equilibrium solubility of CO_2 under the experimental conditions. The diffusion coefficient of CO_2 in the sample was calculated from the slope of M_t/M_∞ plotted against $t^{0.5}/L$. The mPE nanocomposite did not show any distinctively low diffusivity compared with that of mPE, despite the barrier characteristics of nanoparticles reported by others.[11,21–23] Moreover, when the WF was added to the mPE or mPE nanocomposite matrix, there was no distinct difference between the PWC and the PWC nanocomposite.

Flame retardancy

A simple burning test was performed, as shown in Figure 6. The mPE/WF nanocomposites showed enhanced fire retardance. A piece of soft paper was placed on the table, and the rod foam samples were ignited and burned above it. For the mPE/WF composites without clay, the burning sample dripped down quickly and ignited the paper [Fig. 6(a)]. On the contrary, the mPE/WF nanocomposites (5 wt % clay) formed char during burning, without dripping, thus retarding the burning and preventing the fire from spreading [Fig. 6(b)]. The flame-retardancy tests (according to ASTM D 635–03[24]) showed that the burning rate for the mPE/WF nanocomposites was lower than that for the mPE/WF composites (Fig. 7).

CONCLUSIONS

Adding nanoparticles to PWCs increased foam expansion. As expected, the scanning electron microscopy results demonstrated that cell morphology generally improved with respect to the cell size when clay was introduced into plastics. The differential scanning calorimetry results showed that the crystallinity of the mPE/WF nanocomposites varied significantly with the WF content and the clay content. The solubility was well correlated with the crystallinity. The addition of clay did not change the diffusivity of CO_2 in the composites much. Finally, the foam material with clay showed good char formation when it was burned.

References

1. Balatinecz, J. J.; Woodhams, R. T. J Forestry 1993, 91, 22.
2. Chtourou, H.; Riedl, B.; Ait-Kadi, A. J Reinf Plast Compos 1992, 11, 372.
3. Raj, R. G.; Kokta, B. V.; Groleau, G.; Daneault, C. Plast Rubber Process Appl 1989, 11, 215.
4. Matuana, L. M.; Park, C. B.; Balatinecz, J. J. Polym Eng Sci 1998, 38, 1862.
5. Giannelis, E. P. Adv Mater 1996, 8, 29.
6. Okamoto, M.; Nam, P. H.; Maiti, P.; Kotaka, T.; Hasegawa, N.; Usuki, A. Nanoletters 2001, 1, 295.
7. Han, X.; Zeng, C.; Lee, L. J.; Kurt, K. W.; Tomasko, D. L. Soc Plast Eng Annu Tech Conf Tech Pap 2002, 48, 354.
8. Kwak, M.; Lee, M.; Lee, B. K. Soc Plast Eng Annu Tech Conf Tech Pap 2002, 48, 381.
9. Wang, K. H.; Choi, M. H.; Koo, C. M.; Choi, Y. S.; Chung, I. J. Polymer 2001, 42, 9819.
10. Messersmith, P. B.; Giannelis, E. P. J Polym Sci Part A: Polym Chem 1995, 33, 1047.
11. Wunderlich, B.; Czornyj, G. Macromolecules 1977, 10, 906.
12. Rizvi, G. M.; Park, C. B.; Lin, W. S.; Guo, G.; Pop-Iliev, R. Polym Eng Sci 2003, 43, 7, 1347.
13. Guo, G.; Rizvi, G. M.; Park, C. B.; Lin, W. S. J Appl Polym Sci 2004, 91, 621.
14. Myers, G. E.; Kolosic, P. C.; Chahyadi, I.; Coberly, C. A.; Koutsky, J. A.; Ermer, D. S. Proc Mater Res Soc Symp 1990, 197, 67.
15. Colton, J. S.; Suh, N. P. Polym Eng Sci 1987, 27, 500.
16. Naguib, H. E.; Park, C. B.; Reichelt, N. J Appl Polym Sci 2004, 91, 2661.
17. Webb, K. F.; Teja, A. S. Fluid Phase Equilib 1999, 158, 1029.
18. Doroudiani, S.; Park, C. B.; Kortschot, M. T. Polym Eng Sci 1996, 36, 2645.
19. Doroudiani, S.; Park, C. B.; Kortschot, M. T. Polym Eng Sci 1998, 38, 1205.
20. Crank, J.; Park, G. S. Diffusion in Polymers; Academic: New York, 1968.
21. Yano, K.; Usuki, A.; Kurauchi, T.; Kamigaito, O. J Polym Sci Part A: Polym Chem 1993, 31, 2493.
22. Cho, J. W.; Paul, D. R. Polymer 2001, 42, 1083.
23. Usuki, A.; Kojima, Y.; Kawasumi, M.; Okada, A.; Fukushima, Y.; Kurauchi, T.; Kamigaito, O. J Mater Res 1993, 8, 1179.
24. Standard Test Method for Rate of Burning and/or Extent and Time of Burning of Plastics in a Horizontal Position; ASTM D 635-03; ASTM International: West Conshohocken, PA, 2003.